Quantum control of molecular tunneling ionization in the spatiotemporal domain

Hideki Ohmura,[1] Naoaki Saito,[1] and Toru Morishita[2,3]

[1]*National Institute of Advanced Industrial Science and Technology (AIST), 1-1-1 Higashi, Tsukuba, Ibaraki 305-8565, Japan*

[2]*Department of Engineering Science, University of Electro-Communications, 1-5-1 Chofu-ga-oka, Chofu-shi, Tokyo 182-8585, Japan*

[3]*PRESTO, Japan Science and Technology Agency (JST), Sanbancho building, 5-Sanbancho, Chiyodaku, Tokyo 102-0075, Japan*

(Received 9 December 2010; published 13 June 2011)

We report on a method that can control molecular photoionization in both space and time domains. The directionally asymmetric molecular tunneling ionization induced by intense (5.0×10^{13} W/cm^2) phase-controlled two-color laser pulses consisting of fundamental and second-harmonic light achieves the selective ionization of asymmetric molecules in the space domain, and manipulates the birth time and direction of photoelectron emission on an attosecond time scale. This method provides a powerful tool for tracking the quantum dynamics of photoelectrons by using phase-dependent oriented molecules as a phase reference in simultaneous ion-electron detection.

DOI: 10.1103/PhysRevA.83.063407 PACS number(s): 33.80.Rv, 32.80.Qk, 42.50.Hz

I. INTRODUCTION

The quantum dynamics of photoelectrons from molecules generated by intense laser fields, represented by tunneling ionization (TI) and the recollision process that follows [1], plays a key role in very advanced atomic and molecular spectroscopies [2–6]. A recently developed method allows us to capture snapshots of the correlated dynamics of photoelectrons and the spatial orientation of molecules on an attosecond time scale (1 as $= 10^{-18}$ s) [7].

There are two main problems with respect to tracking and manipulating photoelectrons in molecular TI. The first involves manipulation of the quantum dynamics of the photoelectrons in the time domain. Because photoelectrons in TI are generated at the maxima of the oscillating laser fields, tracking and manipulating the motion of photoelectrons requires control on an attosecond time scale [8,9]. Recently, attosecond control of atomic ionization by using phase-stabilized few-cycle laser pulses [10] and an attosecond quantum stroboscope using attosecond extreme-ultraviolet pulses [11] have been reported. However, even with such sophisticated methods, photoelectron emission in both the positive direction and the negative direction along the direction of polarization due to the oscillating laser fields causes mixing between the direct and recollision processes, making the related phenomena complicated [12].

The second principal problem involves the manipulation of molecular orientation in the space domain. Molecules are randomly oriented in the gas and liquid phases, while the light-matter interaction depends on the relative angle between the molecular geometry and the polarization direction of the irradiating light. This angle dependence leads to inhomogeneous molecular control. Recent approaches aimed at overcoming this problem, such as the use of laser-induced molecular alignment and orientation [13] and cold target recoil ion momentum spectroscopy (COLTRIMS) [7], have brought unprecedented progress to the observation of the quantum dynamics of photoelectrons. In particular, COLTRIMS allows us to capture snapshots of the correlated dynamics of photoelectrons and molecular orientation on the attosecond time scale by measuring the three-dimensional (3D) momentum vector of electrons and ions in coincidence [5–7]. However, the use of COLTRIMS for performing coincidence measurements is still limited for various molecular systems in which there are few coincidence events, or too many coincidence events within the dead time of the detector.

Here, we report on a method that can control molecular photoionization in both space and time domains. The directionally asymmetric molecular tunneling ionization induced by intense (5.0×10^{13} W/cm^2) phase-controlled two-color laser pulses consisting of fundamental and second-harmonic light achieves the selective ionization of oriented molecules by discriminating the geometric nature of the wave function in the space domain, and manipulates the birth time and direction of photoelectron emission on an attosecond time scale.

II. EXPERIMENT

Our strategy for the control of molecular TI in the spatiotemporal domain by using phase-controlled two-color laser fields is shown schematically in Fig. 1. TI is induced by removing an electron through the suppressed potential barrier of the combined nuclear and laser fields. Molecular TI can be described by the molecular Ammosov-Delone-Krainov (ADK) model, in which electrons are removed from the highest occupied molecular orbital (HOMO) via the tunneling process [14–17]. According to the molecular ADK model, photoelectrons are much more strongly extracted via the tunneling process from the large-amplitude lobe of the highest occupied molecular orbital (HOMO) along the opposite direction of the electric field vector [14,15]. Consequently, the angle dependence of the ionization rate reflects the geometric structure of the HOMO. Figure 1(a) shows the molecular structure and isocontour of the HOMO of carbon monoxide (CO) determined by *ab initio* calculations [18]. The HOMO of CO shows an asymmetric σ structure. The angular dependence of the TI rate for CO at a laser intensity of 6×10^{13} W/cm^2 reflecting the geometry of the HOMO has been calculated using molecular ADK theory [15,17]. Note that the ionization rate as well as the transverse momentum distribution can be accurately calculated by the recently developed Siegert state method [19]. For monochromatic laser fields with a symmetric waveform, however, electrons are removed at the same rate in both the negative direction and the positive direction along the

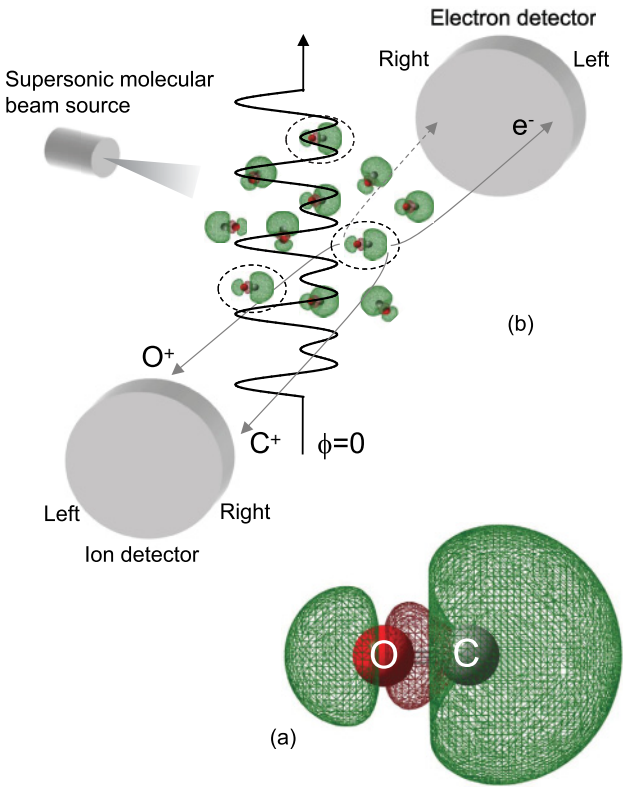

FIG. 1. (Color) (a) Molecular structure and isocontour of the highest occupied molecular orbital (HOMO) of CO. The shading indicates the sign of the wave function. (b) Schematic of the experimental configuration for simultaneous ion-electron detection in directionally asymmetric molecular tunneling ionization (TI) and the principle of selective ionization of oriented molecules (SIOM). The waveform of a phase-controlled two-color $\omega + 2\omega$ laser field at a relative phase difference of $\phi = 0$ is shown by the black solid curve. SIOM (black dotted ellipses) is induced by electron removal from the high-density part of the HOMO opposite to the direction of the electric field vector at its maximum. Trajectories of photofragment ions and photoelectrons are shown by the curved gray arrows.

laser polarization so that single-frequency laser fields cannot discriminate the orientation of C-O from that of O-C [15].

To obtain more control over the manipulation of the photoelectrons, we employ two-color phase-controlled laser fields consisting of a fundamental light and its second harmonic (hereafter, $\omega + 2\omega$ laser field). The total electric field of the linearly polarized $\omega + 2\omega$ laser field is given by $E(t) = E_1 \cos(\omega t) + E_2 \cos(2\omega t + \phi)$, where E_1 and E_2 are the amplitudes of the electric fields and ϕ is the relative phase difference between the ω and 2ω pulses. The phase-controlled $\omega + 2\omega$ field has a characteristic asymmetry: The amplitude of the electric field in the positive (left) direction is twice that in the negative (right) direction when $\phi = 0$ and $E_1 = 2E_2$ [Fig. 1(b)]. The directional asymmetry is reversed when $\phi = \pi$ (not shown). When atoms and molecules are ionized by phase-controlled $\omega + 2\omega$ laser fields, directionally asymmetric TI is expected to be induced. Directionally asymmetric TI was first investigated in atoms [20,21] and was then applied to hydrogen molecules [22]. We have experimentally demonstrated that as a consequence of directionally asymmetric TI of molecules with an asymmetric HOMO, selective ionization of oriented molecules (SIOM) is induced [23–25] [Fig. 1(b)]. SIOM is free of constraints such as the laser wavelength [23,24], pulse duration [23,24], polarity [23], and weight of the molecules [25]. SIOM can be achieved through discrimination of the wave function in the space domain by the enhancement of a nonlinear interaction between the asymmetric laser fields and the asymmetric HOMO structure.

The phase-controlled $\omega + 2\omega$ laser fields can manipulate the birth time and the direction of the photoelectrons within the selected oriented molecules because the directionality of asymmetric TI induced within the attosecond regime is more enhanced for molecules with asymmetric HOMO than for atoms and symmetric molecules by the asymmetric nonlinear interaction. Furthermore, the phase dependence of photofragment ions, which reflects SIOM, works as an accurate phase reference for the quantum dynamics of photoelectrons in simultaneous ion-electron detection. As a result, this method provides an opportunity to observe more unified quantum dynamics of photoelectrons.

The experimental apparatus consisted of a Ti:sapphire laser system [23], a robust phase-controlled $\omega + 2\omega$ laser-field generator [25], and a time-of-flight mass spectrometer (TOF-MS) designed for simultaneous ion-electron detection equipped with a supersonic molecular-beam source. Briefly, the output laser beam of the Ti:sapphire laser system (800-nm wavelength, 130-fs duration, 1.0-mJ/pulse pulse energy, 20-Hz repetition rate) was introduced into the robust phase-controlled $\omega + 2\omega$ laser-field generator [25]. With this device, after second harmonic generation (β-barium borate, type I phase matching, 1-mm thickness, conversion efficiency 30%), we can control the relative phase difference ϕ between the ω and 2ω pulses by using a rotatable 10-mm-thick quartz plate with a resolution of $\sim$30 as (0.05π) [25]. The ratio I_2/I_1 was adjusted to $\sim$0.25 ($E_2/E_1 = 0.5$), where I_1 and I_2 are the intensities of the ω and 2ω pulses, respectively [25]. The relative phase difference was calibrated by simultaneous measurement using the gas mixture of target molecules and reference molecules [23,24].

The phase-controlled $\omega + 2\omega$ laser beam was focused on the supersonic molecular beam of CO [diluted (5%) with He gas, stagnation pressure 0.5 MPa, estimated rotational temperature 20 K] in the TOF-MS by an aluminum concave mirror (200-mm focal length). We estimated the total intensity $I = I_1 + I_2$ to be $\sim 5 \times 10^{13}$ ($I_1 = 4 \times 10^{13}$, $I_2 = 1 \times 10^{13}$ W/cm^2) at the focus.

Simultaneous ion-electron detection in the TOF-MS is shown schematically in Fig. 1(b). The TOF-MS mainly consists of a Wiley-McLaren-type two-stage accelerator, field-free drift regions for electrons and ions, and two opposing position-sensitive detectors. Photofragment ions (photoelectrons) generated by the $\omega + 2\omega$ pulses are accelerated down (up) by static electric fields toward the opposing detectors. The electrode rings used for acceleration incorporate an electrostatic lens to improve the momentum resolution [7]. After passing through a drift tube at an applied voltage of 0 kV for photofragment ions (2.0 kV for photoelectrons), the photofragment ions (photoelectrons) are detected by a position-sensitive detector composed of a microchannel plate (MCP) with a phosphor screen (77 mm in diameter) that was employed to measure both the arrival time and the position

into the MCP detectors. One-dimensional (1D) TOF spectra for photofragment ions were recorded by a digital oscilloscope. Two-dimensional (2D) angular distributions of photofragment ions (photoelectrons) that converted on the position-sensitive detector were recorded by a CCD camera system without a pinhole in front of the MCP detector. Mass selectivity of the fragment ions for the 2D images was achieved by gating the gain of the detector (temporal width 100 ns) at the arrival time of each photofragment ion. In this configuration, we could simultaneously measure the phase dependence of both the photofragment ions and the photoelectrons under identical conditions of the relative phase difference ϕ and laser intensity. The energy resolution of the ion detector (photoelectron detector) was estimated to be 0.1 eV. Our TOF-MS for ion-electron detection is similar to COLTRIMS without a magnetic field [7]. The method does not require coincidence measurements, so it is applicable to molecular systems for which coincidence measurements are difficult to perform.

We define the experimental configuration among the polarization direction, the detection axis, and the direction of electric field maxima at relative phase difference $\phi = 0$. In the measurement of 1D TOF spectra, the polarization direction of the $\omega + 2\omega$ laser fields is set to be horizontal and parallel to the detection axis, and we define $\phi = 0$ to be when the electric field maxima points toward the ion detector [forward-backward configuration (not shown)]. In the measurement of the 2D photofragment (photoelectron) angular distribution, the polarization direction of the $\omega + 2\omega$ laser fields is set to be horizontal and perpendicular to the detection axis, and we define $\phi = 0$ to be when the electric field maxima points leftward (rightward) with respect to the ion (electron) detector [leftward-rightward configuration, shown in Fig. 1(b)].

III. RESULTS AND DISCUSSIONS

Figure 2 shows the TOF mass spectrum of ions when CO molecules were irradiated with $\omega + 2\omega$ pulses in the forward-backward configuration. The generation of singly charged parent CO^+ is the main process (>95%) (Fig. 2, inset). Expanded views of the spectra from singly and doubly photofragmented ions show a pair of peaks, one corresponding to emission directly toward the detector, and the other corresponding to ejection in the backward direction before reversal by the extraction fields. The assignment of each dissociation channel has been reported as a Coulomb explosion process $CO^{(p+q)+} \rightarrow C^{p+} + O^{q+}$ (where p and q are integers) [26]. Strong forward-backward asymmetries show that the C^+ and C^{2+} (O^+ and O^{2+}) ions were preferentially emitted away from (toward) the detector at $\phi = 0$, when the electric field maximum pointed toward the detector. Conversely, the directional asymmetries of each of the photofragments were reversed at $\phi = \pi$. Corresponding 2D angular distributions of the photofragment ions with pronounced angular localization in the leftward-rightward configuration show that a prominent degree of selectivity was achieved both in the orientation direction and in the angular distribution (Fig. 2, images).

The 2D angular distribution of the photoelectrons under irradiation only from the 2ω pulse in the leftward-rightward configuration was observed as a series of clear discrete symmetric ring structures localized in the polarization

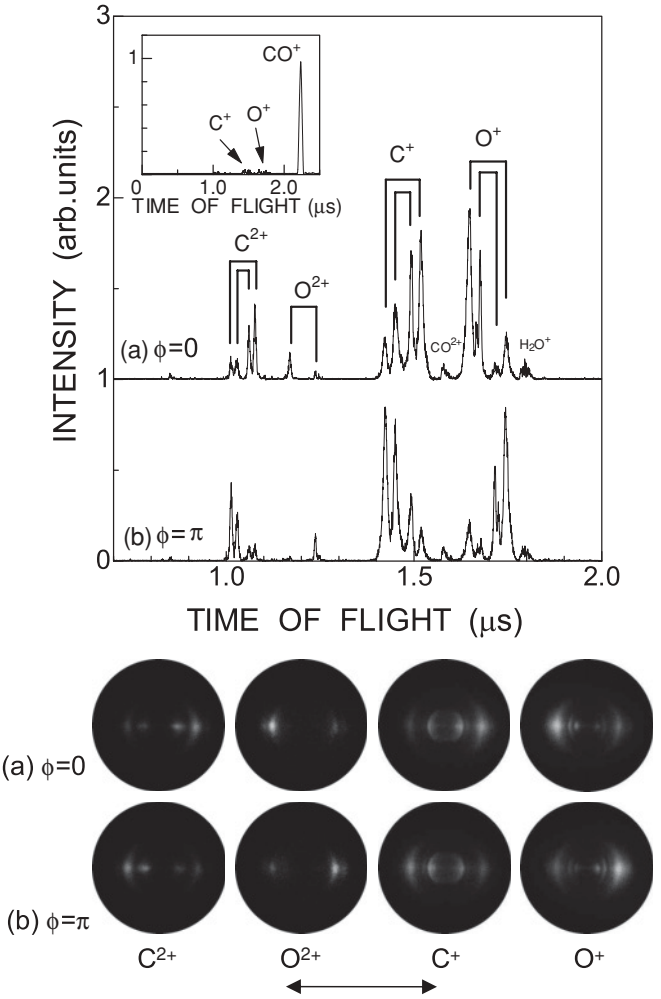

FIG. 2. Graphs: TOF mass spectrum of ions generated by the dissociative ionization of CO molecules irradiated with the phase-controlled $\omega + 2\omega$ laser fields in the forward-backward configuration (inset). Expanded TOF mass spectra of photofragment ions at relative phase differences (a) $\phi = 0$ and (b) $\phi = \pi$. The solid lines indicate pairs of forward and backward peaks. Images: Angular distributions of the photofragment emission generated by the dissociative ionization of CO molecules irradiated with the phase-controlled $\omega + 2\omega$ laser fields in the leftward-rightward configuration at relative phase differences (a) $\phi = 0$ and (b) $\phi = \pi$. The double-headed arrow indicates the direction of polarization.

direction [Fig. 3(a), left-hand column]. In the corresponding photoelectron spectrum as a function of kinetic energy [Fig. 3(a), right-hand column], the energy spacing of the series of peaks is 3.1 eV, which corresponds to the photon energy of the 2ω pulse. This pattern results from the well-known above threshold ionization (ATI), where the lowest peak corresponds to multiphoton ionization (MPI) by overcoming the ionization potential ($I_p = 14.0$ eV), and the subsequent peaks correspond to the absorption of additional photons.

The 2D angular distribution of photoelectrons under irradiation only from the ω pulse was observed as a strongly localized symmetric angular distribution reflecting the polarization of the ω pulse, accompanied by a faint series of discrete ring structures [Fig. 3(b), left-hand column]. In the corresponding photoelectron spectrum, the energy distribution shows a broad

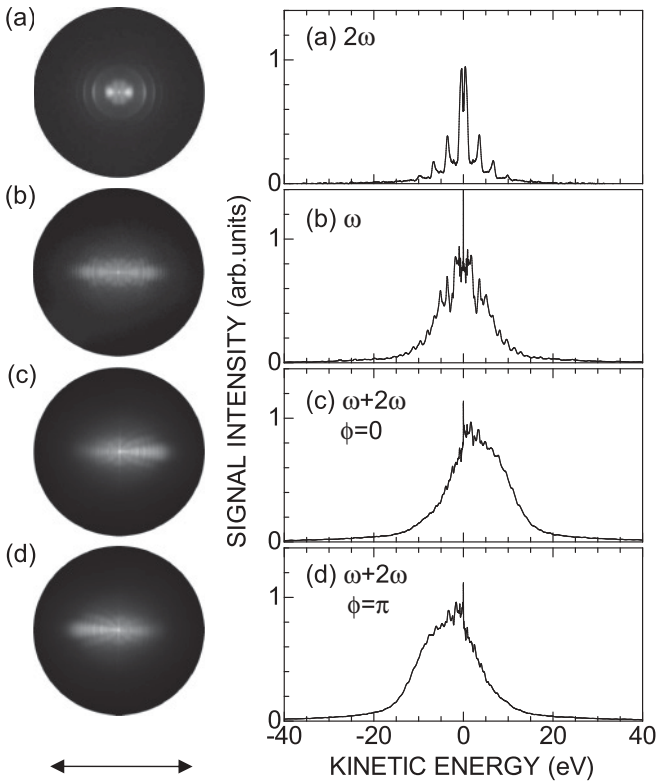

FIG. 3. Images: Angular distributions of photoelectron emission generated by the irradiation of (a) the second harmonic (2ω) lights, (b) the fundamental (ω) lights, and the phase-controlled two-color $\omega+2\omega$ laser fields at relative phase differences (c) $\phi=0$ and (d) $\phi=\pi$. Graphs: Photoelectron spectra as a function of kinetic energy along the polarization direction (double-headed arrow) converted from respective images. Positive (negative) kinetic energy corresponds to rightward (leftward) photoelectron emission.

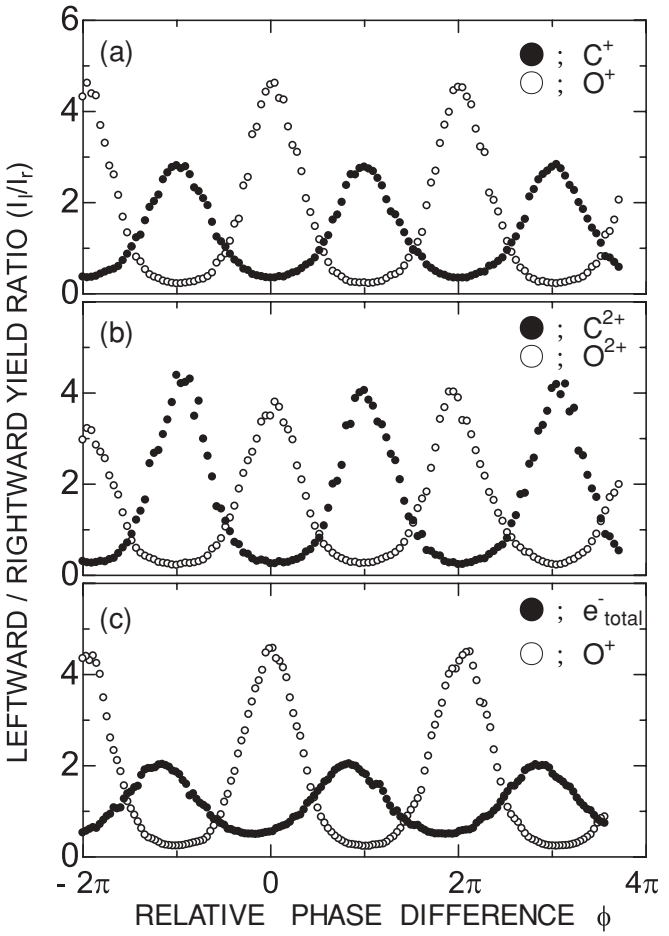

FIG. 4. Leftward-rightward yield ratio (I_l/I_r) of (a) singly charged and (b) doubly charged photofragment ions as a function of relative phase difference ϕ: (closed circles) carbon; (open circles) oxygen. (c) Leftward-rightward yield ratio (I_l/I_r) as a function of relative phase difference ϕ: (open circles) oxygen; (closed circles) total photoelectrons in simultaneous ion-electron detection.

and exponentially decreasing dependence superimposed on a weak series of discrete peaks whose energy spacing is 1.55 eV (half the 2ω irradiation), indicating the transition from MPI to TI [27].

When CO molecules were irradiated by the phase-controlled $\omega+2\omega$ pulses, the intensity of the photoelectron signal became ~10 times the sum of each signal for the ω and the 2ω irradiation due to the highly nonlinear optical process. Figures 3(c) and 3(d) show the 2D angular distribution of photoelectrons and the corresponding photoelectron spectrum at $\phi=0\,(\pi)$. The disappearance of the discrete structures in the photoelectron spectra indicates that the laser intensity reached the TI regime. Furthermore, strong directional asymmetry in the leftward-rightward emission is clearly observed. This asymmetry shows that the photoelectrons were preferentially emitted rightward (leftward) of the electron detector at $\phi=0\,(\pi)$.

A clear periodicity of 2π was observed in the leftward-rightward yield ratio (I_l/I_r) as a function of ϕ for all photofragments displayed (Fig. 4). The phase dependence between $C^+(C^{2+})$ and $O^+(O^{2+})$ indicates they are completely out of phase with each other. This result shows that phase-controlled $\omega+2\omega$ pulses can discriminate the molecular orientation of the head-tail order. Furthermore, the phase dependence between $C^+(O^+)$ and $C^{2+}(O^{2+})$ shows completely in-phase behavior. This indicates that the directions of molecular orientation for singly charged and doubly charged CO are the same.

Most importantly, the quantum dynamics of photoelectrons can be tracked by using the phase-dependent oriented molecules as a phase reference in the simultaneous ion-electron detection. If the photoelectrons are removed via the tunneling process from the large-amplitude lobes of the HOMO opposite to the maxima of the electric fields [hereafter called "intuitive" photoelectron emission following Ref. [28]; the solid gray line of the photoelectron orbit in Fig. 1(b)], the leftward-rightward asymmetry between the O^+ and the photoelectrons is expected to exhibit in-phase behavior. Figure 4(c) shows the I_l/I_r ratio as a function of ϕ in the simultaneous measurement of O^+ and total photoelectrons. The O^+ and photoelectrons are nearly out of phase with each other (the phase lag with respect to O^+ is 0.85π). Experimental results show that the photoelectrons are emitted nearly opposite to the intuitive direction. Figure 5 shows a density plot of the I_l/I_r ratio as a function of ϕ and photoelectron kinetic energy in the simultaneous measurement of O^+ and photoelectrons. The

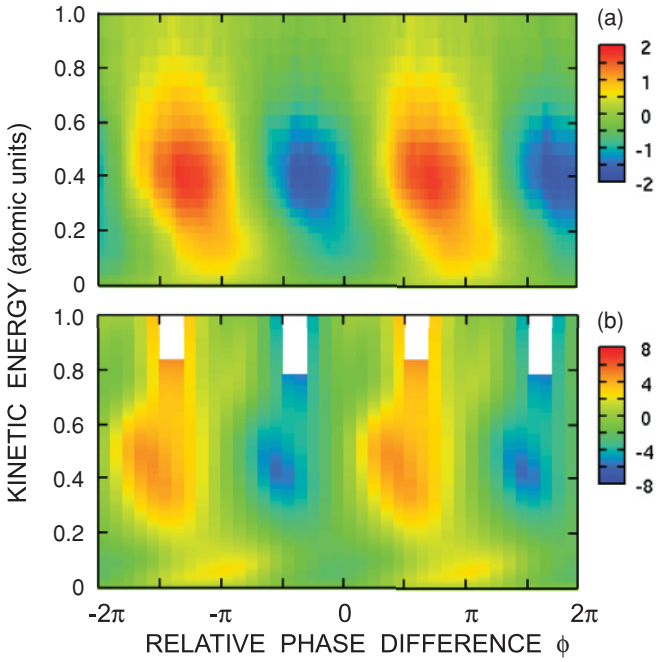

FIG. 5. (Color) Density plot of the leftward-rightward yield ratio (I_l/I_r) for photoelectrons as a function of the relative phase difference ϕ and photoelectron kinetic energy (atomic units): (a) experimental result, (b) numerical calculation. Note that the I_l/I_r ratios are plotted on a log scale.

phase-dependent behavior was dependent on photoelectron kinetic energy, and can be divided into two regions: slow photoelectrons (0–0.3 a.u.) with directional asymmetry at approximately $\phi = 0\,(\pi)$, and fast photoelectrons (0.3–0.7 a.u.) with directional asymmetry at approximately $\phi = \pi/2\,(3\pi/2)$.

We now discuss the quantum dynamics of photoelectrons generated by $\omega + 2\omega$ laser fields. In early studies of photoelectron dynamics generated by irradiation of molecules with intense $\omega + 2\omega$ laser fields, puzzling behavior of the directionally asymmetric emission between positively charged nuclear fragments and photoelectrons was observed [22]. Bandrauk and Chelkowski have discussed theoretically the details of directionally asymmetric photoelectron emission induced by $\omega + 2\omega$ fields [28,29]. First, a two-step model, consisting of quasistatic TI and following the motion of photoelectrons driven by $\omega + 2\omega$ laser fields, predicts no directional asymmetry at $\phi = 0\ (\pi)$ [21,28,29]. Second, they calculated the numerical solution of the time-dependent Schrödinger equation (TDSE) for the 1D H_2^+ molecules and H atoms in phase-controlled $\omega + 2\omega$ laser fields, and found numerically that photoelectrons are emitted opposite to the intuitive direction at $\phi = 0\,(\pi)$. They used an improved two-step model to explain that the origin of the counterintuitive photoelectron emission is the Coulomb attraction from the parent ion [28,29]. Our experimental results can be explained by the two-step model including Coulomb attraction. Current investigations concerning directionally asymmetric photoelectron emission have shifted to the use of few-cycle laser pulses, which also show an asymmetric electric field with the carrier-envelope phase [10,30]. Chelkowski and Bandrauk reached a similar conclusion regarding few-cycle pulses by solving the 3D TDSE for H atoms in which slow photoelectrons, which are more affected by the Coulomb interaction than fast ones, are emitted toward the counterintuitive direction owing to the Coulomb attraction of the parent ion [30]. We have performed a numerical calculation of the 3D TDSE [31]. In brief, we considered a hydrogen atom interacting with a $\omega + 2\omega$ laser field with a pulse-duration of 10 fs, in which asymmetric photoelectron emission induced by the carrier-envelope phase was negligible. The total intensity of the $\omega + 2\omega$ laser field $I = I_1 + I_2$ in the calculation was set to be 5×10^{13} ($I_1 = 4.0 \times 10^{13}$, $I_2 = 1.0 \times 10^{13}$ W/cm^2). To smooth out the ATI peaks, the ratio was obtained by averaging the calculated spectra over bins of $\Delta p = 1.8$ eV. In Fig. 5 the experimental results and the numerical calculation are compared. Our experimental results are qualitatively in agreement with the numerical results obtained by the 3D TDSE, although the absolute value of the I_l/I_r ratio in the experimental results is smaller than that in the numerical calculation, mainly owing to experimentally imperfect conditions such as spatial overlapping between the ω and 2ω laser fields. The experimental results might fail to detect the fine structure seen in the numerical calculation for fast photoelectrons greater than 0.7 a.u. because of the low sensitivity of the electron detector. We can interpret the quantum dynamics of photoelectrons generated by the $\omega + 2\omega$ field by 3D TDSE by connecting with the previously reported two-step model and the improved two-step model. First, the phase-dependent behavior of the slow photoelectrons is in good agreement with the improved two-step model. This result can be explained by the effect in which slow photoelectrons are emitted toward the counterintuitive direction owing to the Coulomb attraction of the parent ion [28,29]. Second, the phase-dependent behavior of the fast photoelectrons approaches asymptotically the two-step model, which predicts directional asymmetry at $\phi = \pi/2\ (3\pi/2)$ [21,28,29]. This result is consistent because fast photoelectrons, which are less affected by the Coulomb interaction than slow ones, are driven by the intense $\omega + 2\omega$ laser fields, shaking off the Coulomb attraction. We have successfully observed the transition from slow photoelectrons to fast electrons in the phase-dependent behavior of directionally asymmetric photoelectron emission induced by the $\omega + 2\omega$ laser field. Finally, the fine structure for fast photoelectrons greater than 0.7 a.u. in the numerical calculation includes the backscattering of photoelectrons by parent ions. Further experimental studies with highly sensitive photoelectron detection are required to examine the very sensitive phase-dependent behavior of the backscattered photoelectrons [12]. Our method provides an opportunity to check the behavior of photoelectrons in TI for various molecules by quantum calculations by using both the numerical approach of 3D TDSE, taking into account the Stark-shift-corrected strong field approximation [32] and an analytical approach such as Coulomb-corrected strong-field approximation theory [33] for quantitative understanding.

IV. CONCLUSION

We have investigated the directionally asymmetric molecular tunneling ionization induced by intense phase-controlled two-color laser pulses consisting of fundamental and second-harmonic lights. The most important improvement

in our present experiment is the ideal combination of the asymmetric wave form of the $\omega + 2\omega$ field and asymmetric molecules with large asymmetric HOMO, which is based on knowledge that we gained in our previous work [23–25]. By selecting the ideal combination, phase-controlled $\omega + 2\omega$ laser fields can more effectively manipulate the birth time and the direction of the photoelectrons within the selected oriented molecules because the directionality of the induced asymmetric TI is more enhanced for molecules with asymmetric HOMO than for atoms and symmetric molecules, owing to the asymmetric nonlinear interaction. This ideal situation has been confirmed by the present experimental results in which the phase dependence of the directionality of asymmetric TI is huge. As a result, by selecting the ideal combination, we have successfully observed the transition from slow electrons to fast electrons in the phase-dependent behavior of directionally asymmetric photoelectron emission induced by the $\omega + 2\omega$ field. In previous studies of molecular ionization induced by phase-controlled $\omega + 2\omega$ laser fields, it has often been controversial as to how to calibrate the relative phase difference ϕ [34–36]. This method provides a powerful tool for tracking the quantum dynamics of photoelectrons by using phase-dependent oriented molecules as a phase reference in simultaneous ion-electron detection.

ACKNOWLEDGMENTS

This work was partially supported by the Precursory Research for Embryonic Science and Technology (PRESTO) program of the Japan Science and Technology Agency (JST) and a Grant-in-Aid for Young Scientists (A) as well as a Grant-in-Aid for scientific research (C) from the Japan Society for the Promotion of Science (JSPS).

[1] P. B. Corkum, Phys. Rev. Lett. **71**, 1994 (1993).
[2] H. Niikura, F. Légaré, R. Hasbani, M. Y. Ivanov, D. M. Villeneuve, and P. B. Corkum, Nature (London) **421**, 826 (2003).
[3] J. Itatani, J. Levesque, D. Zeidler, H. Niikura, H. Pépin, J. C. Kieffer, P. B. Corkum, and D. M. Villeneuve, Nature (London) **432**, 867 (2004).
[4] T. Kanai, S. Minemoto, and H. Sakai, Nature (London) **435**, 470 (2005).
[5] M. Meckel *et al.*, Science **320**, 1478 (2008).
[6] T. Morishita, A.-T. Le, Z. Chen, and C. D. Lin, Phys. Rev. Lett. **100**, 013903 (2008).
[7] J. Ullrich, R. Moshammer, A. Dorn, R. Dörner, L. Ph. H. Schmidt, and H. Schmidt-Böcking, Rep. Prog. Phys. **66**, 1463 (2003).
[8] M. Uiberacker *et al.*, Nature (London) **446**, 627 (2007).
[9] P. Eckle, A. N. Pfeiffer, C. Cirelli, A. Staudte, R. Dörner, H. G. Muller, M. Büttiker, and U. Keller, Science **322**, 1525 (2008).
[10] G. G. Paulus, F. Lindner, H. Walther, A. Baltuška, E. Goulielmakis, M. Lezius, and F. Krausz, Phys. Rev. Lett. **91**, 253004 (2003).
[11] J. Mauritsson, P. Johnsson, E. Mansten, M. Swoboda, T. Ruchon, A. L'Huillier, and K. J. Schafer, Phys. Rev. Rett. **100**, 073003 (2008).
[12] O. I. Tolstikhin, T. Morishita, and S. Watanabe, Phys. Rev. A **81**, 033415 (2010).
[13] V. Kumarappan, L. Holmegaard, C. Martiny, C. B. Madsen, T. K. Kjeldsen, S. S. Viftrup, L. B. Madsen, and H. Stapelfeldt, Phys. Rev. Lett. **100**, 093006 (2008).
[14] X. M. Tong, Z. X. Zhao, and C. D. Lin, Phys. Rev. A **66**, 033402 (2002).
[15] C. D. Lin and X. M. Tong, J. Photochem. Photobiol. A **182**, 213 (2006).
[16] A. S. Alnaser, S. Voss, X.-M. Tong, C. M. Maharjan, P. Ranitovic, B. Ulrich, T. Osipov, B. Shan, Z. Chang, and C. L. Cocke, Phys. Rev. Lett. **93**, 113003 (2004).
[17] Song-Feng Zhao, Cheng Jin, Anh-Thu Le, T. F. Jiang, and C. D. Lin, Phys. Rev. A **81**, 033423 (2010).
[18] M. J. Frisch *et al.*, *Gaussian 03, Revision C.02* (Gaussian, Inc., Wallingford, CT, 2004).
[19] P. A. Batishchev, O. I. Tolstikhin, and T. Morishita, Phys. Rev. A **82**, 023416 (2010).
[20] K. J. Schafer and K. C. Kulander, Phys. Rev. A **45**, 8026 (1992).
[21] D. W. Schumacher, F. Weihe, H. G. Muller, and P. H. Bucksbaum, Phys. Rev. Lett. **73**, 1344 (1994).
[22] B. Sheehy, B. Walker, and L. F. DiMauro, Phys. Rev. Lett. **74**, 4799 (1995).
[23] H. Ohmura, N. Saito, and M. Tachiya, Phys. Rev. Lett. **96**, 173001 (2006).
[24] H. Ohmura and M. Tachiya, Phys. Rev. A **77**, 023408 (2008).
[25] H. Ohmura, N. Saito, H. Nonaka, and S. Ichimura, Phys. Rev. A **77**, 053405 (2008).
[26] J. Lavancier, D. Normand, C. Cornaggia, J. Morellec, and H. X. Liu, Phys. Rev. A **43**, 1461 (1991).
[27] E. Mevel, P. Breger, R. Trainham, G. Petite, and P. Agostini, Phys. Rev. Lett. **70**, 406 (1993).
[28] A. D. Bandrauk and S. Chelkowski, Phys. Rev. Lett. **84**, 3562 (2000).
[29] S. Chelkowski, M. Zamojski, and A. D. Bandrauk, Phys. Rev. A **63** 023409 (2001).
[30] S. Chelkowski and A. D. Bandrauk, Phys. Rev. A **71**, 053815 (2005).
[31] T. Morishita, Z. Chen, S. Watanabe, and C. D. Lin, Phys. Rev. A **75**, 023407 (2007).
[32] M. Abu-samha and L. B. Madsen, Phys. Rev. A **82**, 043413 (2010).
[33] S. V. Popruzhenko, G. G. Paulus, and D. Bauer, Phys. Rev. A **77**, 053409 (2008).
[34] S. De *et al.*, Phys. Rev. Lett. **103**, 153002 (2009).
[35] D. Ray *et al.*, Phys. Rev. Lett. **103**, 223201 (2009).
[36] K. J. Betsch, D. W. Pinkham, and R. R. Jones, Phys. Rev. Lett. **105**, 223002 (2010).